Review Article Brain Conflux

Multiscale Modeling of Transcranial Alternating Current Stimulation: Induced Electric Field and Cellular Responses

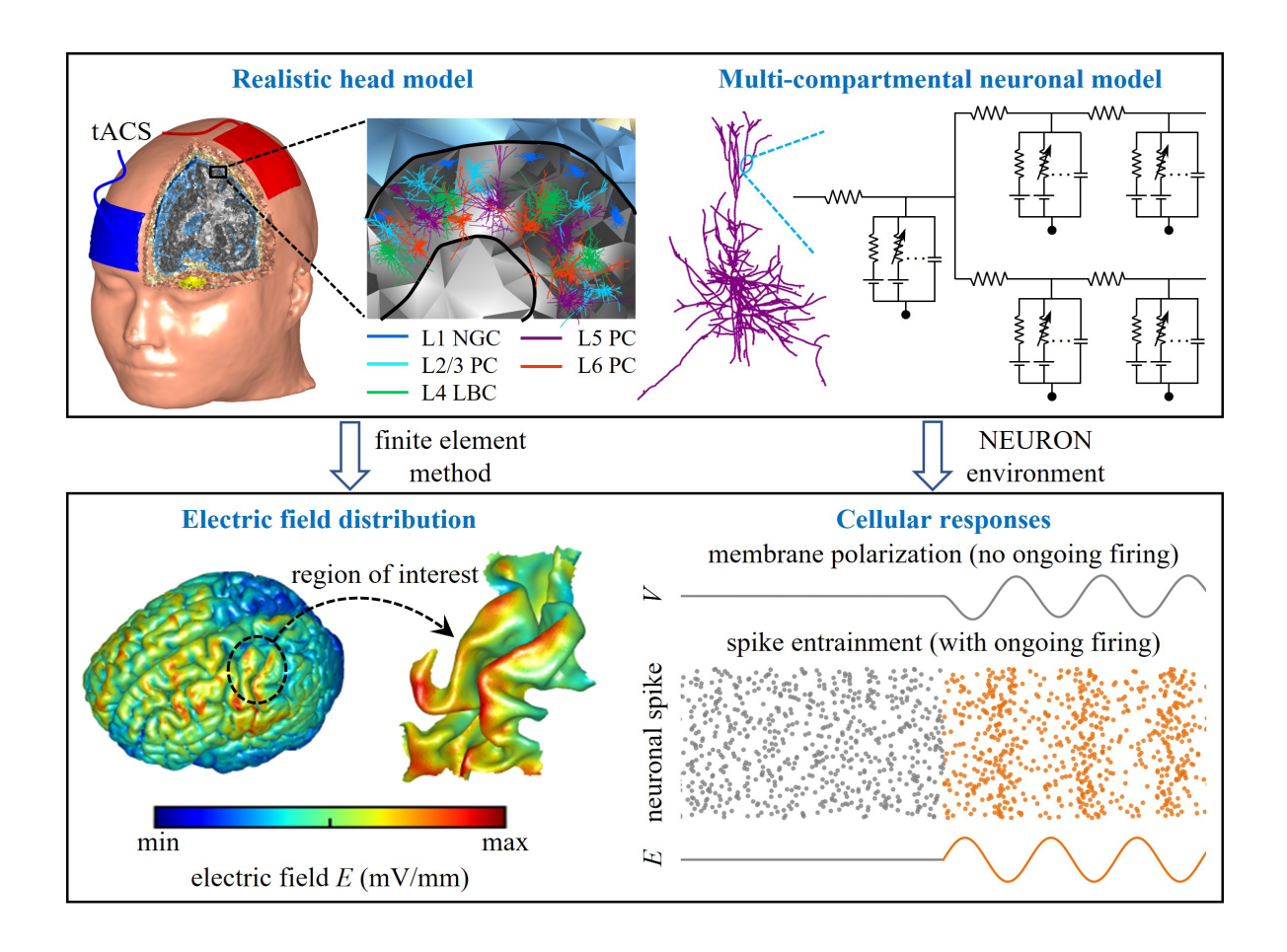
Authors

Guosheng Yi, Xinbo Hou, Xuelin Huang, Fu Zhang, Jintao Chen, Shen Li

Correspondence

lishen@tmu.edu.cn (S. Li)

Graphical Abstract



Review Article Brain Conflux

Multiscale Modeling of Transcranial Alternating Current Stimulation: Induced Electric Field and Cellular Responses

Guosheng Yi¹, Xinbo Hou¹, Xuelin Huang¹, Fu Zhang¹, Jintao Chen¹, Shen Li^{2,3*}

Received: 2025-09-20 | Accepted: 2025-10-19 | Published online: 2025-11-11

Abstract

Transcranial alternating current stimulation (tACS) is a non-invasive neuromodulation technique that generates weak oscillatory electric fields (EFs) in the brain and has shown promise for probing neural oscillations and treating neuropsychiatric disorders. However, its effects on neural activity remain highly variable across studies, and controversies persist regarding whether conventional tACS intensities can genuinely entrain neuronal firing. Experimental approaches alone have limited capacity to resolve these inconsistencies. Computational modeling provides a powerful complementary framework to quantify induced EFs, predict cellular responses, and generate mechanistic hypotheses. In this review, we focus on multiscale models spanning from macroscopic realistic head models to microscopic multi-compartmental neuronal models. Head models elucidate how anatomy, tissue conductivity, stimulation parameters, and electrode montage shape the spatial distribution of tACS-induced fields, while multi-compartmental models reveal how EFs, neuronal morphology, biophysics, and synaptic inputs govern cell-type-specific polarization and spike entrainment. We highlight key insights, unresolved controversies, and emerging trends, including the integration of head and neuronal models, network-level simulations, and the use of artificial intelligence to bridge scales. By critically synthesizing advances in multiscale modeling, we argue that coupling computational frameworks with experimental recordings is essential for explaining the diversity of tACS effects and for translating mechanistic insights into individualized, clinically effective interventions.

Keywords: Transcranial alternating current stimulation; computational modeling; induced electric field; multi-compartmental neuronal models; membrane polarization; spike entrainment.

Introduction

Transcranial alternating current stimulation (tACS) uses scalp electrodes to apply low-intensity current (typically no more than 2 mA) at a specific frequency to modulate neural activity in a noninvasive and tolerable manner [1, 2]. By targeting endogenous oscillations, tACS provides a unique opportunity to probe the causal relationship between neural oscillations, cognition, and behavior [3, 4], and it is increasingly explored as a therapeutic strategy for neuropsychiatric disorders [5-7]. Despite rapid growth in experimental and clinical applications, the mechanisms by which tACS shapes neural dynamics remain incompletely understood.

At the core of tACS action are oscillatory electric fields (EFs) generated within the brain [8]. Such field is the acting force for driving its effects on neural activity [3]. The weak oscillatory field induced by tACS is not strong enough to activate action potentials in resting neurons, which is traditionally categorized

as a subthreshold stimulation. Experimental recordings in rats [9-13], ferrets [14, 15], nonhuman primates [16-20], and humans [13] showed that such weak EFs can modulate spike timing and entrain neural activity. The above interventions are determined by EF strength and frequency, which also depend on cell type and ongoing oscillations. Particularly, tACS-induced effects on neural activity are highly variable across studies, and some findings are not fully reliable and difficult to replicate. This inconsistency has fueled ongoing debate over whether conventional tACS intensities, commonly 1-2 mA at the scalp, can genuinely entrain neural firing in vivo [21-24]. Computational modeling has emerged as a powerful complement to experimental approaches for addressing these controversies. Models can quantify EF distributions across tissues, test mechanistic hypotheses at the cellular level, and guide experimental design and clinical protocols [25-26]. In particular, realistic head models allow estimation of EF distribution across brain regions based on individual anatomy, while

^{*} Corresponding Author.



¹ School of Electrical and Information Engineering, Tianjin University, Tianjin, 300072, China.

² Brain Assessment & Intervention Laboratory, Tianjin Anding Hospital, Mental Health Center, Tianjin Medical University, Tianjin, 300222, China

³ Institute of Mental Health, Tianjin Anding Hospital, Mental Health Center, Tianjin Medical University, Tianjin, 300222, China

multi-compartmental neuronal models capture the morphology- and biophysics-dependent responses of single cells to applied fields. Integrating these scales enables mechanistic insights into how tACS affects neural activity, from the distribution of currents in the brain to the entrainment of individual neurons.

Previous studies [2-5, 8, 27-31] summarized the neurophysiological and cognitive effects of tACS and discussed methodological challenges. In contrast, our review focuses specifically on multiscale computational modeling. We first outline advances in realistic head models that predict EF distributions, then examine multi-compartmental neuronal models that characterize cellular polarization and spiking entrainment. Finally, we discuss how integrating these approaches can resolve current controversies, highlight emerging directions such as network-level and artificial intelligence-assisted modeling, and consider the implications for translating tACS into individualized, clinically effective neuromodulation.

Realistic Head Models of tACS

tACS generates oscillating EFs across brain tissues, which are usually measured in units of voltage per meter (V/m) or millivolts per millimeter (mV/mm) [3, 32]. As noted, the fluctuating EF is the acting force of tACS. Therefore, calculation of EF in the target region is a first step to mechanistically understand cellular responses via modeling. Measured EFs can also be used to facilitate electrode montage selection and individualized dosing [3, 33, 34], and to predict inter-individual variability in tACS effects [35].

Realistic head models are powerful tools for predicting EF distribution induced in the brain during tACS [36, 37], which are often impractical to measure using experimental methods alone. These head models are created from anatomical magnetic resonance imaging (MRI), segmented into different tissue types such as scalp, skull, cerebrospinal fluid, gray matter. and white matter. The typical workflow includes MRI segmentation, 3D-surface tissue reconstruction, electrode placement, volume mesh generation, assignment of electrical conductivity and permittivity, specification of physics settings and boundary conditions, and finite element method (FEM) calculation [36, 38]. Common toolboxes used for simulating EF in realistic head models include SimNIBS [39, 40], COMETS2 [41], ROAST [38], SCIRun [42], and SimBio [43]. These toolboxes use FEM to numerically calculate EFs. Note that when calculating tACS-induced fields, it is usually assumed that the coupling between electric and magnetic fields is negligible, i.e., the quasi-static approximation [44]. This approximation is valid in the frequency range currently used for tACS [45].

The calculation of EF induced by tACS depends on the electrical conductivity of brain tissues. Since tissue conductivity varies between individuals, it is necessary to validate the predictions of a head model with *in vivo* measurements. Huang et al [46] directly measured EF in ten epilepsy patients generated by tACS and calibrated individual head models by adjusting skull, scalp, and brain conductivities to match recorded EFs. The resulting individualized models predicted EF spatial distribution with high accuracy for all subjects. Their validation results were later confirmed by Opitz et al [47], which consistently showed that realistic brain models using standard

conductivities slightly misestimate the measured EF strength, suggesting the need for individual adjustments of tissue conductivities. Further, tissue conductivity exhibits inter-individual variability, and accounting for this variation is crucial for gaining better insights into stimulation mechanisms. However, many tACS modeling studies are based on a single exemplary head model. To capture anatomical and tissue variabilities, Berger et al [48] recently created a comprehensive dataset of 100 quality-assured realistic head models with variable tissue conductivities based on individual imaging data from the Human Connectome Project s1200 release. To reflect inter-individual variability, the scalp, skull, and grey matter tissue conductivities for each model were assigned pseudo-randomly from biologically plausible distributions [49]. The cerebrospinal fluid, white matter, and eye tissue conductivities were fixed at the default setting. To assess the quality of each head mesh, the authors performed a semi-manual correction for tissue accuracy and quality measurements of finite-element analysis. They also provided the simulation results of exemplary tACS montage based on a desynchronized montage outlined by Alekseichuk et al [50]. The dataset of their head models can assist in population variability analysis, meta-modeling techniques, and stimulation target optimization.

Other factors affecting tACS-induced EF distribution include stimulation current intensity, frequency, phase, electrode placement, and head anatomy. Recordings in surgical epilepsy patients [46] showed that the maximum EF exhibits approximately linear dependence on stimulation current intensity, which is about 0.4-0.5 V/m in human when current intensity is 1 mA from peak-to-baseline. Recordings in monkeys [32] showed that there is a small attenuation (up to 10%) in EF intensity as stimulation frequency increases. Alekseichuk et al [51] combined direct invasive recordings with computational models to characterize the dependence of EF magnitude and phase on stimulation phase during multi-electrode tACS. Their work demonstrated that specific phase configurations can create a "traveling wave" stimulation pattern, in which the location of maximum EF shifts over time. Subsequently, Lee et al [52] used phasor algebra and detailed head models to develop a simulation framework for predicting the phase gradient of EFs during multi-channel tACS. Their simulations precisely predicted in vivo recordings in monkeys when the return electrode was placed within a small radius (< 5 mm) from its actual location. They individually calibrated the overestimation in EF amplitude through optimization of tissue conductivity, which enhanced the correspondence between simulated and measured field amplitudes. Using validated head models, Opitz et al [47] determined the tolerance limits for variation in electrode placement, recommending that a placement accuracy of within 1 cm is required for reliable tACS application. In a following comparative modeling study involving mice, monkeys, and humans [53], the same research group revealed that head size is another factor influencing EF strength. Moreover, Ma et al [54] identified skull thickness, scalp thickness, and epidural cerebrospinal fluid thickness as key anatomical factors that contribute to the inter-individual variability of EF intensity.

Multi-Compartmental Neuronal Models of Cellular Responses to tACS

The oscillatory EF generated by tACS with conventional intensities (i.e., 1-2 mA) can periodically polarize the transmembrane potential. In vitro recordings in rats showed that such polarization response almost linearly increases with EF strength and decreases substantially as field frequency is varied from 10 Hz to 100 Hz [10]. The mean sensitivity of membrane potential to applied field exhibits an exponential decay function of frequency. However, other in vitro experiments in rats [9, 13] and humans [13] reported there is no frequency dependence in membrane polarization by weak EFs. Additionally, consistent evidence from in vitro studies in rats [9, 10, 12, 13], ferrets [14], and humans [13], as well as in vivo recordings in rats [11], ferrets [14, 15] and nonhuman primates [16-20] showed that the weak EF can alter neural spike timing and cause entrainment. Yet, the degree of entrainment is highly variable within and across cell types. Some in vivo experiments in humans [23, 24] even revealed that the current intensities commonly used may not be sufficient to genuinely entrain neural activity. These contradictory findings underscore the necessity of using computational models to quantify and understand the variable effects of tACS on cellular activity.

Multi-Compartmental Neuronal Models

The neural response to tACS is not only determined by the induced EF but also depends on cell properties, including biophysics, morphology, orientation, and ongoing brain activity. Using EF distribution alone is not sufficient to predict all cellular effects of tACS, which should be coupled to single-neuron models. Multi-compartmental models are powerful tools for predicting cellular responses to spatially distributed EF. This type of model discretizes the complex cell morphology into small compartments. Each compartment includes its specific membrane capacitance, resistance, ionic channel, and morphological features (i.e., length and diameter). Adjacent compartments are connected by an intracellular (axial) resistance. The membrane potential gradient along the neurites generates axial currents flowing between compartments. The branch points in the dendrites or axon connect to at least three neighboring compartments. The conductance-based models introduced by Hodgkin and Huxley [55] provide powerful tools for describing the relationship between electrical activity and underlying ionic currents in each compartment. According to Hodgkin-Huxley (HH) formalism, an ionic current is calculated as the product of its conductance and driving force. See reference [56] for a more comprehensive description of such mod-

The multi-compartmental conductance-based neuronal models with realistic morphologies have been developed and validated for a wide range of cell types across animal species and humans, which are publicly available through repositories such as ModelDB, GitHub, and the library of Blue Brain models. A common software for simulating compartmental models is the NEURON environment [57], which offers a user-friendly graphical interface. It also allows users to develop custom models, execute simulations, and optimize parameters using Python, MATLAB or its specific programming language based on hoc.

tACS is modeled by applying the induced EF to each cell compartment as its extracellular voltage using NEURON's extracellular mechanism [58-60]. The spatial morphologies of multi-compartmental models allow them to effectively describe the biophysical effects of EF on cell membrane. Since large current sources generated by the electrode placed at the scalp are distant from underlying cells, the induced EF has a low spatial gradient at the scale of individual neurons [61, 62]. Thus, when introducing the EF generated by a scalp electrode to a neuronal model, the field is often assumed to be uniform, i.e., the quasi-uniform assumption [59, 61-63].

According to the HH framework, transmembrane potential dynamics emerge from the interactions of intrinsic membrane properties, which include passive capacitance-resistance and voltage-gated ionic conductances [56]. These properties collectively govern cellular filtering behaviors over a range of stimulation frequencies. When an oscillatory EF is applied, it modulates transmembrane voltage by altering the extracellular potential in each neuronal compartment. Such periodic perturbations interact with the membrane time constant and ion channel kinetics, thereby conferring an inherent frequency dependence on cellular response to oscillatory EFs.

Modeling Studies on Membrane Polarization

Membrane polarization is the subthreshold response of resting neurons to weak EFs, which significantly depends on cell morphology and stimulation frequency. Multi-compartmental HH-type models have been used to simulate tACS-induced membrane polarization (summarized in Table 1). Under the quasi-uniform assumption, these studies directly apply weak sinusoidal EFs to isolated neuronal models without synaptic input or other external stimuli.

Computational studies have examined the frequency-dependent polarization response in subcellular elements of neocortical layer 5 pyramidal cells (L5 PCs), including dendrites, soma, and axon. Toloza et al [59] applied weak sinusoidal EFs to a multi-compartmental PC model, and field intensity is limited to 5 mV/mm peak-to-peak to make sure cellular response is subthreshold. They found that the membrane polarization in the apical dendrites is opposite to the soma and basal dendrites. When the apical region is depolarized, the basal region is hyperpolarized, and vice versa. Membrane polarization depends on field orientation relative to the cell, and the maximal polarization occurs when the EF is parallel to the somato-dendritic axis. These simulations are consistent with earlier modeling [64] and in vitro [65] results. Membrane response is also shaped by EF frequency. The polarization in the apical tuft exhibits a frequency resonance at 20 ± 4 Hz, corresponding to a band-pass behavior. The polarization in other cell compartments decreases monotonically with increasing stimulation frequency, exhibiting a low-pass filter behavior. The hyperpolarization-activated cation current (I_b) is the primary ionic mechanism that leads to the resonance response in distal dendrites, and its conductance density controls the resonance frequency. Subsequently, Aspart et al [66] used multi-compartmental models to quantify the frequency-dependent polarization profile in the dendrites and soma of a L5b PC to AC fields of sinusoidal waveform. They calculated cell sensitivity to AC fields by the ratio of polarization amplitude to field amplitude. In their simulations, the field sensitivity in apical dendrites exhibits a frequency resonance around 10-20 Hz, which is not observed in the soma or basal dendrites. They related these differential frequency-dependent polarization profiles to cell morphology and active channels. The former increases field sensitivity in the apical dendrites, while the presence of high density of h-type channels decreases field sensitivity at low field frequencies. We recently used two-compartment models to analyze the membrane polarization induced by oscillating EFs in the frequency domain [67]. We applied linear system analysis to compute the transfer functions of the models, which were then used to understand the frequency-dependent patterns of membrane polarization. We showed that the presence of I_b introduces a new zero and pole to dendritic transfer function, reducing polarization amplitude at low frequencies and causing a visible frequency resonance. We also found that the compartment geometry, internal coupling conductance, and other ionic currents affect the polarization response mainly by altering the gain and poles of transfer functions.

Membrane polarization has also been quantified in different types of cells. Tran et al [60] examined somatic polarization in L1 neurogliaform cell (NGC), L2/3 PC, L4 large basket cell (LBC), L5 PC, and L6 PC using multi-compartmental models with oscillatory EFs. They applied polarization length to quantify cell sensitivity to applied EF, which was computed by somatic polarization per unit field. They showed that there is a linear relationship between somatic polarization and EF strength. and the mean coefficient of determination R2 is 0.9818 over the set of all neurons. L5 PC exhibits the highest polarization lengths, followed by L6 PC and L2/3 PC. L1 NGC and L4 LBC have lower values than PCs. Recently, we used a set of multi-compartmental models to examine the polarization response in the subcellular elements of above five cell types to sinusoidal EFs [68]. For each cell type, we included five virtual clones with random variations in their dendritic and axonal morphologies, which were previously validated to replicate cellular responses to weak fields [61]. Our simulations showed that membrane polarization varies by cell type and subcellular element. The somatic polarization in PCs is sensitive to sinusoidal EF that is oriented roughly parallel to the cortical column, while the polarization sensitivity to field direction for

non-pyramidal cells varies between clones. Axon usually exhibits the highest polarization, followed by the dendrites and soma. For PCs, the polarization in the apical dendrites exhibits a visible frequency resonance, while the other subcellular elements primarily exhibit low-pass behavior. These findings are consistent with above mentioned studies [59, 66, 67]. The subcellular elements of non-pyramidal cells exhibit complex frequency-dependent polarization profiles. Similarly, Gaugain et al [69] found that somatic polarization in PCs is the highest at direct current and decreases exponentially with AC frequency, which corresponds to a low-pass filter behavior. The polarization in inhibitory neurons exhibits a resonance in the 5-15 Hz range. L5 PCs have the highest polarization lengths, and somatostatin and parvalbumin cells have lower values.

Modeling Studies on Entrainment of Spiking Activity

The subthreshold membrane polarization by tACS can alter spike timing and entrain neural activity. The multi-compartmental HH-type models have also been used to examine these effects on ongoing firing activity (summarized in Table 2). In this scenario, the synaptic inputs are applied to multi-compartmental models to generate spontaneous firing. The neural entrainment is commonly quantified by phase locking value (PLV), which measures spike timing synchronization relative to tACS waveform [60, 69]. The minimum PLV is 0, which means the spike timings are uniformly distributed over all phases. The maximum value is 1, which means the spike timing is perfectly synchronized to a specific phase of tACS.

Computational studies have investigated spike entrainment by tACS in different types of cortical cells. In these studies, tACS was modeled by directly applying a spatially uniform EF with sinusoidal waveform to an isolated multi-compartmental model. Using this method, Tran et al [60] systematically examined the effects of tACS on firing activity in L1 NGC, L2/3 PC, L4 LBC, L5 PC, and L6 PC. To generate spontaneous firing activity, an excitatory synaptic input was added to each cell at a random location on the apical dendrite for PCs or the basal dendrite for interneurons. A stochastic Poisson process was used to model the presynaptic input. The synaptic conductance

Table 1. Summary of Multi-compartmental Modeling Studies on Membrane Polarization.

| Reference | Cortical Cell Type | Main Results | |
|--------------------|--|---|--|
| Toloza et al [59] | L5 PC | ${\sf I}_{\sf h}$ is the primary ionic mechanism that leads to the resonance response to tACS in the apical dendrites. | |
| Aspart et al [66] | L5 PC | Cell morphology and $\mbox{\it I}_{\mbox{\tiny h}}$ contribute to the resonance in the apical dendrites. | |
| Huang et al [67] | PC | Passive membrane properties and I_{h} underlie frequency-dependent polarization by altering the model's transfer function. | |
| Tran et al [60] | L1 NGC, L2/3 PC, L4 LBC, L5 PC, L6 PC | L5 PC exhibits the highest polarization lengths, followed by L6 PC and L2/3 PC. L1 NGC and L4 LBC have lower values than PCs. | |
| Huang et al [68] | L1 NGC, L2/3 PC, L4 LBC, L5 PC, L6 PC | Membrane polarization varies by cell type and subcellular element. Axon usually exhibits the highest polarization, followed by the dendrites and soma. | |
| Gaugain et al [69] | L2/3 PC, L5 PC, L6 PC, VIP interneurons, SST interneurons, PV interneurons | Somatic polarization in PCs decreases with frequency, which exhibits a resonance in inhibitory neurons. L5 PCs have the highest polarization lengths, and SST and PV cells have lower values. | |

was modeled using a two-exponential function. They found that sine-wave EF does not alter the firing rate of cortical cells when field intensity is in the range of human experiments (i.e., < 1 V/m). However, such weak fields can entrain the spiking activity in L5 PC and L4 LBC. L2/3 and L6 PCs exhibit weaker entrainment than L5 PC and L4 LBC, and no entrainment is observed in L1 NGC. The cell-type-specific entrainment is related to neuronal morphology and cell biophysics. Recently, Gaugain et al [69] found that the phase entrainment of cortical cells is dependent on EF intensity and frequency. In their simulations, the presynaptic spike train was also generated by a stochastic Poisson distribution. The multiple synapses and their parameters were determined to generate reproducible firing activity with a mean rate at 10 Hz in each cell. They showed that there is a linear increase in entrainment to tACS frequency with EF intensity. When EF intensity is 10 V/m, L5 PCs exhibit the highest entrainment at their intrinsic firing frequency, which decays with stimulus frequency. The entrainment in inhibitory neurons increases with frequency. They also developed three-compartment PC model and single-compartment inhibitory neuron model to replicate above simulations. These simplified models can be used for faster computation of network-level dynamics with tACS.

To mechanistically understand the morphology-dependent effects of tACS, several studies [70, 71] employed integrate-and-fire (IF) models to approximate neural activity generated in a biophysically more sophisticated ball-and-stick (BS) model. The BS model consists of a lumped somatic compartment attached to a passive dendritic cable with a specified length. The IF model provides a simple phenomenological description of spike generation while retaining biologically plausibility of HH-type dynamics [72]. In IF models, a spike is generated when membrane potential exceeds a predefined threshold. Aspart et al [70] developed extended IF models to reflect the morphology-dependent EF effects extracted from a BS model. The in vivo like noisy synaptic inputs were used to generate spontaneous spiking, which were modeled as Ornstein-Uhlenbeck processes. They found that an oscillatory EF causes spike rate resonance and the resonance frequency depends on synaptic input location, which is related to the dendritic filter of synaptic inputs. With the similar technique, Ladenbauer and Obermayer [71] analytically determined the parameters of a two-compartment model to reproduce somatic voltage dynamics in a BS model. The IF formalism was used to model the spike dynamics in each compartment. They found that the oscillatory EF (1 V/m) causes a clear resonance in spike rate when its frequency is in the beta and low gamma bands. They further showed that the weak field effectively reflects anti-correlated inputs at the soma and dendrite, which modulate firing activity and lead to spike rate resonance. Using the two-compartment models described above, we recently investigated the effects of oscillatory EFs on spike train correlations between pairs of unconnected neurons driven by shared fluctuating dendritic inputs [73]. We observed that output correlation increases with EF intensity while exhibits resonance at specific field frequencies. This correlation resonance is influenced by the morphological differences between the somatic and dendritic compartments, with increased structural asymmetry resulting in more pronounced resonant behavior. These findings were further validated using morphologically detailed PC models.

An isolated multi-compartmental model cannot account for all cellular effects of tACS, and it is necessary to examine cellular responses to stimulation in a neuronal network with synaptic connections. Multi-compartmental models incorporate numerous variables, parameters, and nonlinearities. Incorporating these models into networks with synaptic connections to simulate cellular responses thus significantly increases computational cost. For this reason, simpler neuronal models are often appropriate for network-scale simulations of tACS. The relevant HH-type model usually includes two compartments, which is the minimal individual neuronal unit to capture the spatial polarization by EFs [71, 73, 74]. One compartment represents the apical dendrite, and the other compartment is the soma. Particularly, they are still computationally efficient when simulating network dynamics. The method for coupling EF to a two-compartment model is the same as that used in multi-compartmental models. With the network of two-compartmental models, Zhao et al [75] found that low intensity tACS (< 0.3 V/m) desynchronizes neural firing relative to ongoing endogenous oscillations, while higher intensity stimulation (> 0.3 V/m) directly entrains neural firing. These are consistent with experimental recordings in the nonhuman primate brain [20]. Compared to isolated single cells, tACS-induced entrainment is amplified by synaptic coupling and network effects. Their simulations also revealed that oscillatory EFs directly entrain pyramidal cell and then drive the interneurons. Note that the two-compartment models do not include realistic cell morphology, which is an important factor that may lead to variability in single neuron responses to tACS [60, 66, 70]. Importantly, such simplified models are unable to simulate membrane polarization in dendritic and axonal terminals as well as their arbors, and thus neglect tACS effects on presynaptic and postsynaptic compartments [61]. All these factors can affect their predictions on input-output properties in single neurons and further alter network-level activity. Simulation of tACS effects on large-scale networks with morphologically detailed neuronal models can be executed on the supercomputers [61. 76]. Further, there were studies using networks of phenomenological models (such as, Izhikevich or IF models) to simulate the entrainment of cortical oscillations by tACS, which were reviewed in reference [27] and not covered here.

Above studies use a uniform EF to describe tACS, which do not consider the anatomical distribution of EFs. Wischnewski et al [19] integrated multi-compartmental models of L5 thick-tufted PCs with a realistic head model to simulate tACS effects on spiking activities. Alternating currents were applied to the scalp anterior and posterior of motor cortex through two electrodes. The head model predicts that the EF is strongest at crown of the precentral gyrus, which is 0.31 mV/mm and decreases with depth into the sulcus. Such EF significantly entrains L5 PCs without altering firing rates. The neural entrainment by tACS depends on the orientation of cortical cells. Since the locations of PCs in anterior and posterior wall of the precentral gyrus are along electric current direction, they are more entrained than those at the crown and the bottom of the sulcus. Further, the anterior wall and posterior wall are entrained at different phases. Wischnewski et al [19] also developed a simplified microcircuit model with two PCs and one interneuron, and each neuron was described by a two-compartment model consisting of a soma and a dendrite. Combined with the realistic head model, they replicated the phase shifts over time observed in experimental recordings, suggesting that N-methyl-D-aspartate (NMDA)-mediated synaptic plasticity is a factor that drives above phase precession. We recently used multiscale modeling to examine how L5 PCs in primary motor cortex respond to conventional M1-SO tACS [77]. The simulations of an anatomically accurate head model showed that the induced EFs distribute heterogeneously across the L5 surface of interest. By calculating PLV and preferred phase of

morphologically realistic neuronal models, we found that the direction and intensity of heterogeneous EF and cell morphology are factors that contribute to the diverse entrainments. Our simulations also validated the quasi-uniform assumption used for modeling tACS effects on spike entrainment. The synaptic inputs in above two studies are modeled using a similar approach to Tran et al [60]. Note that such multiscale models were also applied to quantify the axonal and dendritic

Table 2. Summary of Multi-compartmental Modeling Studies on Entrainment of Spiking Activity.

| Reference | Neuronal Model | tACS Model | Main Results |
|----------------------------------|--|--|--|
| Tran et al [60] | isolated multi-compart- mental model with realistic morphology | uniformly distributed sinusoidal EF | Weak fields (< 1 V/m) entrain spiking activity in L5 PC and L4 LBC. L2/3 and L6 PCs exhibit weaker entrainment than L5 PC and L4 LBC, and no entrainment is observed in L1 NGC. Cell-type-specific entrainment is related to neuronal morphology and biophysics. |
| Gaugain et al [69] | isolated multi-compart- mental model with realistic morphology | uniformly distributed sinusoidal EF | Phase entrainment depends on EF intensity and frequency. L5 PCs exhibit the highest entrainment at 10 Hz when field intensity is 10 V/m, which decays with stimulus frequency. The entrainment in inhibitory cells increases with frequency. |
| Aspart et al [70] | extended IF model developed based on a BS model | uniformly distributed sinusoidal EF | An oscillatory EF causes spike rate resonance and the resonance frequency depends on synaptic input location, which is related to the dendritic filter for synaptic inputs. |
| Ladenbauer and Obermayer [71] | two-compartment IF model developed based on a BS model | uniformly distributed sinusoidal EF | An oscillatory EF (1 V/m) effectively reflects anti-cor- related inputs at the soma and dendrite, which modu- late firing activity and lead to spike rate resonance. |
| Huang et al [73] | two-compartment IF model developed based on a BS model | uniformly distributed sinusoidal EF | Spike train correlation increases with EF intensity while exhibits resonance at specific field frequencies. This correlation resonance is influenced by the morphological differences between the somatic and dendritic compartments. |
| Zhao et al [75] | cortical network consisting of 800 PCs and 200 inter- neurons, and each neuron is described by a two-com- partment HH-type model | uniformly distributed sinusoidal EF | Low intensity EF (< 0.3 V/m) desynchronizes neural firing relative to ongoing endogenous oscillations, while higher intensity field (> 0.3 V/m) directly entrains neural firing. tACS-induced entrainment is amplified by synaptic coupling and network effects. The oscillatory EFs directly entrain PCs and then drive the interneurons. |
| Wischnewski et al [19] | isolated multi-compart- mental model with realistic morphology | EFs calculated in a realistic head model | EF entrains L5 PCs without altering firing rates, which depends on the orientation of cortical cells. The PCs in anterior and posterior wall of the precentral gyrus are more entrained than those at the crown and the bottom of the sulcus. |
| Wischnewski et al [19] | a microcircuit with two PCs and one interneuron, and each neuron is described by a two-compartment HH- type model | EFs calculated in a realistic head model | NMDA-mediated synaptic plasticity is a factor that drives the phase shifts over time observed in experimental recordings. |
| Huang et al [77] | isolated multi-compart- mental model with realistic morphology | EFs calculated in a realistic head model | EF heterogeneity and cell morphology are factors that contribute to diverse entrainments. The quasi-uniform assumption used for modeling tACS effects on spike entrainment is validated. |

polarization by transcranial direct current stimulation [61] and cortical neuron activation by transcranial magnetic stimulation [78]. These studies collectively indicate that the multiscale modeling is a promising approach for understanding cellular response to noninvasive brain stimulation.

Conclusions

tACS offers a noninvasive means to probe and modulate neural oscillations, yet fundamental questions remain about its ability to entrain neuronal activity at conventionally applied intensities. Multiscale computational models provide a critical framework for resolving these controversies by linking macroscopic EF distributions to cell-type-specific polarization and spike entrainment. Realistic head models have clarified how anatomy, tissue conductivity, stimulation parameters, and electrode montage shape field strength, while multi-compartmental neuronal models have demonstrated how cell morphology, ionic currents, and synaptic inputs govern cellular responsiveness.

Data-driven methods have been applied to develop multiscale models to reproduce and integrate experimental data. Markram et al [76] used a multi-objective optimization to constrain the vector of ion channel conductance densities in neocortical microcircuitry to reproduce recorded spike features. Dura-Bernal et al [79] applied a hyperparameter optimization framework to tune synaptic weights in auditory thalamocortical circuits to produce physiological firing rates. The resulting data-driven multiscale models were used to interpret the cellular and circuit mechanisms underlying experimental observations. Therefore, the data-driven integration of multiscale models with experimental recordings across species and human neuroimaging will be essential for identifying cell- and region-specific mechanisms of tACS, reconciling translational differences, and capturing excitatory-inhibitory network interactions.

Further, the convolutional neural networks were previously used to rapidly predict EF distribution in brain tissues [80-81] and activation threshold in cortical cells [82] during transcranial magnetic stimulation. The temporal convolutional networks were applied to predict the subthreshold dynamics and spike timing in L5 PCs with synaptic inputs [83]. The hierarchical convolutional neural networks were used to model neural single-unit and population responses in higher visual cortical areas [84]. These studies suggest that artificial neural networks could be introduced to assist in multiscale tACS modeling and bridge the data at different scales. By advancing toward individualized, validated, and clinically informed modeling frameworks, potentially enhanced by artificial intelligence technologies, future work can transform tACS from a variable experimental tool into a precise neuromodulation strategy with robust therapeutic applications.

Abbreviations

VIP: vasoactive intestinal peptide; SST: somatostatin; PV: parvalbumin.

Author Contributions

GSY contributed to conceptualization, literature review, supervision, manuscript writing, and revision. XBH and XLH contributed to literature review, manuscript writing, and revision. FZ and JTC contributed to literature review and revision. SL contributed to conceptualization, literature review, manuscript writing, and revision.

Acknowledgements

Not applicable.

Ethics Approval and Consent to Participate

Not applicable.

Funding information

This work was sponsored by National Natural Science Foundation of China (82371512), Natural Science Foundation of Tianjin (24JCYBJC01000), Tianjin Health Research Project (TJWJ2024MS037) and Tianjin Key Medical Discipline Construction Project (TJYXZDXK-3-015B). All funding had no role in study design, data analysis, paper submission and publication.

Competing Interests

The authors declare that they have no existing or potential commercial or financial relationships that could create a conflict of interest at the time of conducting this study.

Data Availability

All data needed to evaluate the conclusions in the paper are present in the paper or the Supplementary Materials. Additional data related to this paper may be requested from the authors.

References

- [1] Antal A, Paulus W. (2013). Transcranial alternating current stimulation (tACS). Front Hum Neurosci, 7, 317. http://doi.org/10.3389/fnhum.2013.00317
- [2] Van Hoornweder S, Stagg CJ, Wischnewski M. (2025). Personalizing transcranial electrical stimulation. Trends Neurosci, 48(9), 663-678. https://doi.org/10.1016/ j.tins.2025.07.007
- [3] Wischnewski M, Alekseichuk I, Opitz A. (2023). Neurocognitive, physiological, and biophysical effects of transcranial alternating current stimulation. Trends Cogn Sci, 27(2),189-205. https://doi.org/10.1016/j.tics.2022.11.013
- [4] Riddle J, Frohlich F. (2021). Targeting neural oscillations

- with transcranial alternating current stimulation. Brain Res, 1765, 147491. https://doi.org/10.1016/j.brain-res.2021.147491
- [5] Agboada D, Zhao Z, Wischnewski M. (2025). Neuroplastic effects of transcranial alternating current stimulation (tACS): from mechanisms to clinical trials. Front Hum Neurosci, 19, 1548478. https://doi.org/10.3389/fn-hum.2025.1548478
- [6] Gholamali Nezhad F, Martin J, Tassone VK, Swiderski A, Demchenko I, Khan S, et al. (2024). Transcranial alternating current stimulation for neuropsychiatric disorders: a systematic review of treatment parameters and outcomes. Front Psychiatry, 15, 1419243. https://doi.org/10.3389/ fpsyt.2024.1419243
- [7] Biačková N, Adamová A, Klírová M. (2024). Transcranial alternating current stimulation in affecting cognitive impairment in psychiatric disorders: a review. Eur Arch Psychiatry Clin Neurosci, 274(4), 803-826. https://doi.org/10.1007/s00406-023-01687-7
- [8] Liu A, Vöröslakos M, Kronberg G, Henin S, Krause MR, Huang Y, et al. (2018). Immediate neurophysiological effects of transcranial electrical stimulation. Nat Commun, 9(1), 5092. https://doi.org/10.1038/s41467-018-07233-7
- [9] Anastassiou CA, Perin R, Markram H, Koch C. (2011). Ephaptic coupling of cortical neurons. Nat Neurosci, 14(2), 217-23. https://doi.org/10.1038/nn.2727
- [10] Deans JK, Powell AD, Jefferys JG. (2007). Sensitivity of coherent oscillations in rat hippocampus to AC electric fields. J Physiol, 583(Pt 2), 555-65. https://doi.org/10.1113/jphysiol.2007.137711
- [11] Ozen S, Sirota A, Belluscio MA, Anastassiou CA, Stark E, Koch C, et al. (2010). Transcranial electric stimulation entrains cortical neuronal populations in rats. J Neurosci, 30(34), 11476-85. https://doi.org/10.1523/JNEUROS-CI.5252-09.2010
- [12] Francis JT, Gluckman BJ, Schiff SJ. (2003). Sensitivity of neurons to weak electric fields. J Neurosci, 23(19), 7255-61. https://doi.org/10.1523/JNEUROS-CI.23-19-07255.2003
- [13] Lee SY, Kozalakis K, Baftizadeh F, Campagnola L, Jarsky T, Koch C, et al. (2024). Cell-class-specific electric field entrainment of neural activity. Neuron, 112(15), 2614-2630. e5. https://doi.org/10.1016/j.neuron.2024.05.009
- [14] Fröhlich F, McCormick DA. (2010). Endogenous electric fields may guide neocortical network activity. Neuron, 67(1), 129-43. https://doi.org/10.1016/j.neuron.2010.06.005
- [15] Huang WA, Stitt IM, Negahbani E, Passey DJ, Ahn S, Davey M, et al. (2021). Transcranial alternating current stimulation entrains alpha oscillations by preferential phase synchronization of fast-spiking cortical neurons to stimulation waveform. Nat Commun, 12(1), 3151. https://doi.org/10.1038/s41467-021-23021-2
- [16] Krause MR, Vieira PG, Csorba BA, Pilly PK, Pack CC. (2019). Transcranial alternating current stimulation entrains single-neuron activity in the primate brain. Proc Natl Acad Sci U S A, 116(12), 5747-5755. https://doi.org/10.1073/pnas.1815958116
- [17] Vieira PG, Krause MR, Pack CC. (2020). tACS entrains neural activity while somatosensory input is blocked. PLoS Biology, 18(10), e3000834. https://doi.org/10.1371/journal.

- pbio.3000834
- [18] Johnson L, Alekseichuk I, Krieg J, Doyle A, Yu Y, Vitek J, et al. (2020). Dose-dependent effects of transcranial alternating current stimulation on spike timing in awake nonhuman primates. Sci Adv, 6(36), eaaz2747. https://doi.org/10.1126/sciadv.aaz2747
- [19] Wischnewski M, Tran H, Zhao Z, Shirinpour S, Haigh ZJ, Rotteveel J, et al. (2024). Induced neural phase precession through exogenous electric fields. Nat Commun, 15(1), 1687. https://doi.org/10.1038/s41467-024-45898-5
- [20] Krause MR, Vieira PG, Thivierge JP, Pack CC. (2022). Brain stimulation competes with ongoing oscillations for control of spike timing in the primate brain. PLoS Biol, 20(5), e3001650. https://doi.org/10.1371/journal.pbio.3001650
- [21] Beliaeva V, Polania R. (2020). Can low-intensity tACS genuinely entrain neural activity in vivo? Brain Stimul, 13(6), 1796-1799. https://doi.org/10.1016/j.brs.2020.10.002
- [22] Khatoun A, Asamoah B, Mc Laughlin M. (2019). How does transcranial alternating current stimulation entrain single-neuron activity in the primate brain? Proc Natl Acad Sci U S A, 116(45), 22438-22439. https://doi.org/10.1073/ pnas.1912927116
- [23] Vöröslakos M, Takeuchi Y, Brinyiczki K, Zombori T, Oliva A, Fernández-Ruiz A, et al. (2018). Direct effects of transcranial electric stimulation on brain circuits in rats and humans. Nat Commun, 9(1), 483. https://doi.org/10.1038/ s41467-018-02928-3
- [24] Lafon B, Henin S, Huang Y, Friedman D, Melloni L, Thesen T, et al. (2017). Low frequency transcranial electrical stimulation does not entrain sleep rhythms measured by human intracranial recordings. Nat Commun, 8(1), 1199. https://doi.org/10.1038/s41467-017-01045-x
- [25] Zuidema W, French RM, Alhama RG, Ellis K, O'Donnell TJ, Sainburg T, et al. (2020). Five ways in which computational modeling can help advance cognitive science: lessons from artificial grammar learning. Top Cogn Sci, 12(3), 925-941. https://doi.org/10.1111/tops.12474
- [26] Aberra AS, Peterchev AV, Grill WM. (2018). Biophysically realistic neuron models for simulation of cortical stimulation. J Neural Eng, 15(6), 066023. https://doi.org/10.1088/1741-2552/aadbb1
- [27] Madadi Asl M, Valizadeh A. (2025). Entrainment by transcranial alternating current stimulation: Insights from models of cortical oscillations and dynamical systems theory. Phys Life Rev, 53, 147-176. https://doi.org/10.1016/j.plrev.2025.03.008
- [28] Bland NS, Sale MV. (2019). Current challenges: the ups and downs of tACS. Exp Brain Res, 237(12), 3071-3088. https://doi.org/10.1007/s00221-019-05666-0
- [29] Beliaeva V, Savvateev I, Zerbi V, Polania R. (2021). Toward integrative approaches to study the causal role of neural oscillations via transcranial electrical stimulation. Nat Commun, 12(1), 2243. https://doi.org/10.1038/s41467-021-22468-7
- [30] Sasaki R. (2025). Modulating cortico-cortical networks with transcranial alternating current stimulation: a minireview. Phys Ther Res, 28(1), 1-8. https://doi.org/10.1298/ptr. R0035
- [31] He Y, Liu S, Chen L, Ke Y, Ming D. (2023). Neurophysiological mechanisms of transcranial alternating current stimulation. Front Neurosci, 17, 1091925. https://doi.

- org/10.3389/fnins.2023.1091925
- [32] Opitz A, Falchier A, Yan CG, Yeagle EM, Linn GS, Megevand P, et al. (2016). Spatiotemporal structure of intracranial electric fields induced by transcranial electric stimulation in humans and nonhuman primates. Sci Rep, 6, 31236. https://doi.org/10.1038/srep31236
- [33] Sadeghihassanabadi F, Misselhorn J, Gerloff C, Zittel S. (2022). Optimizing the montage for cerebellar transcranial alternating current stimulation (tACS): a combined computational and experimental study. J Neural Eng, 19(2), 026060. https://doi.org/10.1088/1741-2552/ac676f
- [34] Van Hoornweder S, Cappozzo V, De Herde L, Puonti O, Siebner HR, Meesen RLJ, et al. (2024). Head and shoulders-The impact of an extended head model on the simulation and optimization of transcranial electric stimulation. Imaging Neurosci (Camb), 2, imag-2-00379. https://doi.org/10.1162/imag_a_00379
- [35] Kasten FH, Duecker K, Maack MC, Meiser A, Herrmann CS. (2019). Integrating electric field modeling and neuroimaging to explain inter-individual variability of tACS effects. Nat Commun, 10(1), 5427. https://doi.org/10.1038/ s41467-019-13417-6
- [36] Miranda PC, Callejón-Leblic MA, Salvador R, Ruffini G. (2018). Realistic modeling of transcranial current stimulation: the electric field in the brain. Curr Opin Biomed Eng, 8, 20-27. https://doi.org/10.1016/j.cobme.2018.09.002
- [37] Hunold A, Haueisen J, Nees F, Moliadze V. (2023). Review of individualized current flow modeling studies for transcranial electrical stimulation. J Neurosci Res, 101(4), 405-423. https://doi.org/10.1002/jnr.25154
- [38] Huang Y, Datta A, Bikson M, Parra LC. (2019). Realistic volumetric-approach to simulate transcranial electric stimulation-ROAST-a fully automated open-source pipeline. J Neural Eng, 16(5), 056006. https://doi.org/10.1088/1741-2552/ab208d
- [39] Thielscher A, Antunes A, Saturnino GB. (2015). Field modeling for transcranial magnetic stimulation: a useful tool to understand the physiological effects of TMS? Conf Proc IEEE Eng Med Biol Soc, 2015, 222-225. https://doi.org/10.1109/EMBC.2015.7318340
- [40] Nielsen JD, Madsen KH, Puonti O, Siebner HR, Bauer C, Madsen CG, et al. (2018). Automatic skull segmentation from MR images for realistic volume conductor models of the head: Assessment of the state-of-the-art. Neuroimage, 174, 587-598. https://doi.org/10.1016/j.neuroimage.2018.03.001
- [41] Lee C, Jung YJ, Lee SJ, Im CH. (2017). COMETS2: An advanced MATLAB toolbox for the numerical analysis of electric fields generated by transcranial direct current stimulation. J Neurosci Methods, 277, 56-62. https://doi. org/10.1016/j.jneumeth.2016.12.008
- [42] Dannhauer M, Brooks D, Tucker D, MacLeod R. (2012). A pipeline for the simulation of transcranial direct current stimulation for realistic human head models using SCIRun/BioMesh3D. Annu Int Conf IEEE Eng Med Biol Soc, 2012, 5486-5489. https://doi.org/10.1109/EMBC.2012.6347236
- [43] Wagner S, Rampersad SM, Aydin Ü, Vorwerk J, Oostendorp TF, Neuling T, et al. (2014). Investigation of tDCS volume conduction effects in a highly realistic head model. J Neural Eng, 11(1), 016002. https://doi.org/10.1088/1741-

- 2560/11/1/016002
- [44] Ruffini G, Wendling F, Merlet I, Molaee-Ardekani B, Mekonnen A, Salvador R, et al. (2013). Transcranial current brain stimulation (tCS): models and technologies. IEEE Trans Neural Syst Rehabil Eng, 21(3), 333-45. https://doi.org/10.1109/TNSRE.2012.2200046
- [45] Gaugain G, Quéguiner L, Bikson M, Sauleau R, Zhadobov M, Modolo J, et al. (2023). Quasi-static approximation error of electric field analysis for transcranial current stimulation. J Neural Eng, 20(1), 016027. https://doi.org/10.1088/1741-2552/acb14d
- [46] Huang Y, Liu AA, Lafon B, Friedman D, Dayan M, Wang X, et al. (2017). Measurements and models of electric fields in the in vivo human brain during transcranial electric stimulation. Elife, 6, e18834. https://doi.org/10.7554/eLife.18834
- [47] Opitz A, Yeagle E, Thielscher A, Schroeder C, Mehta AD, Milham MP. (2018). On the importance of precise electrode placement for targeted transcranial electric stimulation. Neuroimage, 181, 560-567. https://doi.org/10.1016/ j.neuroimage.2018.07.027
- [48] Berger TA, Wischnewski M, Opitz A, Alekseichuk I. (2025). Human head models and populational framework for simulating brain stimulations. Sci Data, 12(1), 516. https://doi.org/10.1038/s41597-025-04886-0
- [49] McCann H, Pisano G, Beltrachini L. (2019). Variation in reported human head tissue electrical conductivity values. Brain Topogr, 32(5), 825-858. https://doi.org/10.1007/ s10548-019-00710-2
- [50] Alekseichuk I, Pabel SC, Antal A, Paulus W. (2017). Intrahemispheric theta rhythm desynchronization impairs working memory. Restor Neurol Neurosci, 35(2), 147-158. https://doi.org/10.3233/RNN-160714
- [51] Alekseichuk I, Falchier AY, Linn G, Xu T, Milham MP, Schroeder CE, et al. (2019). Electric field dynamics in the brain during multi-electrode transcranial electric stimulation. Nat Commun, 10(1), 2573. https://doi.org/10.1038/s41467-019-10581-7
- [52] Lee S, Shirinpour S, Alekseichuk I, Perera N, Linn G, Schroeder CE, et al. (2023). Predicting the phase distribution during multi-channel transcranial alternating current stimulation in silico and in vivo. Comput Biol Med, 166, 107516. https://doi.org/10.1016/j.compbiomed.2023.107516
- [53] Alekseichuk I, Mantell K, Shirinpour S, Opitz A. (2019). Comparative modeling of transcranial magnetic and electric stimulation in mouse, monkey, and human. Neuroimage, 194, 136-148. https://doi.org/10.1016/j.neuroimage.2019.03.044
- [54] Ma WW, Wang FX, Yi YY, Huang Y, Li XY, Liu YO, et al. (2024). Mapping the electric field of high-definition transcranial electrical stimulation across the lifespan. Sci Bull, 69(24), 3876-3888. https://doi.org/10.1016/j.scib.2024.10.001
- [55] Hodgkin AL, Huxley AF. (1952). A quantitative description of membrane current and its application to conduction and excitation in nerve. J Physiol, 117(4), 500-44. https:// doi.org/10.1113/jphysiol.1952.sp004764
- [56] David S, Bruce G, Andrew G, editor. Principles of computational modelling in neuroscience. 1st ed. New York: Cambridge University Press; 2011.
- [57] Hines ML, Carnevale NT. (1997). The NEURON simulation environment. Neural Comput, 9(6), 1179-209. https://doi.

- org/10.1162/neco.1997.9.6.1179
- [58] Anastassiou CA, Montgomery SM, Barahona M, Buzsáki G, Koch C. (2010). The effect of spatially inhomogeneous extracellular electric fields on neurons. J Neurosci, 30(5), 1925-1936. https://doi.org/10.1523/JNEUROS-CI.3635-09.2010
- [59] Toloza EHS, Negahbani E, Fröhlich F. (2018). In interacts with somato-dendritic structure to determine frequency response to weak alternating electric field stimulation. J Neurophysiol, 119(3), 1029-1036. https://doi.org/10.1152/ jn.00541.2017
- [60] Tran H, Shirinpour S, Opitz A. (2022). Effects of transcranial alternating current stimulation on spiking activity in computational models of single neocortical neurons. Neuroimage, 250, 118953. https://doi.org/10.1016/j.neuroimage.2022.118953
- [61] Aberra AS, Wang R, Grill WM, Peterchev AV. (2023). Multi-scale model of axonal and dendritic polarization by transcranial direct current stimulation in realistic head geometry. Brain Stimul, 16(6), 1776-1791. https://doi.org/10.1016/j.brs.2023.11.018
- [62] Bikson M, Dmochowski J, Rahman A. (2013). The "quasi-uniform" assumption in animal and computational models of non-invasive electrical stimulation. Brain Stimul, 6(4), 704-705. https://doi.org/10.1016/j.brs.2012.11.005
- [63] Jackson MP, Rahman A, Lafon B, Kronberg G, Ling D, Parra LC, et al. (2016). Animal models of transcranial direct current stimulation: Methods and mechanisms. Clin Neurophysiol, 127(11), 3425-3454. https://doi.org/10.1016/j.clinph.2016.08.016
- [64] Radman T, Ramos RL, Brumberg JC, Bikson M. (2009). Role of cortical cell type and morphology in subthreshold and suprathreshold uniform electric field stimulation in vitro. Brain Stimul, 2(4), 215-228.e3. https://doi.org/10.1016/j.brs.2009.03.007
- [65] Bikson M, Inoue M, Akiyama H, Deans JK, Fox JE, Miyakawa H, et al. (2004). Effects of uniform extracellular DC electric fields on excitability in rat hippocampal slices in vitro. J Physiol, 557(Pt 1), 175-190. https://doi.org/10.1113/ jphysiol.2003.055772
- [66] Aspart F, Remme MWH, Obermayer K. (2018). Differential polarization of cortical pyramidal neuron dendrites through weak extracellular fields. PLoS Comput Biol, 14(5), e1006124. https://doi.org/10.1371/journal.pcbi.1006124
- [67] Huang X, Wang J, Yi G. (2024). Frequency-domain analysis of membrane polarization in two-compartment model neurons with weak alternating electric fields. Cogn Neurodyn, 18(3), 1245-1264. https://doi.org/10.1007/s11571-023-09980-w
- [68] Huang X, Wei X, Wang J, Yi G. (2024). Frequency-dependent membrane polarization across neocortical cell types and subcellular elements by transcranial alternating current stimulation. J Neural Eng, 21(1), 016034. https://doi.org/10.1088/1741-2552/ad2b8a
- [69] Gaugain G, Al Harrach M, Yochum M, Wendling F, Bikson M, Modolo J, et al. (2025). Frequency-dependent phase entrainment of cortical cell types during tACS: computational modeling evidence. J Neural Eng, 22(1), 016028. https:// doi.org/10.1088/1741-2552/ad9526
- [70] Aspart F, Ladenbauer J, Obermayer K. (2016). Extending integrate-and-fire model neurons to account for the effects

- of weak electric fields and input filtering mediated by the dendrite. PLoS Comput Biol, 12(11), e1005206. https://doi.org/10.1371/journal.pcbi.1005206
- [71] Ladenbauer J, Obermayer K. (2019). Weak electric fields promote resonance in neuronal spiking activity: Analytical results from two-compartment cell and network models. PLoS Comput Biol, 15(4), e1006974. https://doi. org/10.1371/journal.pcbi.1006974
- [72] Brette R. (2015). What is the most realistic single-compartment model of spike initiation?. PLoS Comput Biol, 11(4), e1004114. https://doi.org/10.1371/journal.pcbi.1004114
- [73] Huang X, Wei X, Wang J, Yi G. (2025). Effects of transcranial alternating current stimulation on spike train correlation in two-compartment model neurons. Biol Cybern, 119(4-6), 26. https://doi.org/10.1007/s00422-025-01025-1
- [74] Yi GS, Wang J, Wei XL, Tsang KM, Chan WL, Deng B, et al. (2014). Exploring how extracellular electric field modulates neuron activity through dynamical analysis of a two-compartment neuron model. J Comput Neurosci, 36(3), 383-399. https://doi.org/10.1007/s10827-013-0479-z
- [75] Zhao Z, Shirinpour S, Tran H, Wischnewski M, Opitz A. (2024). Intensity- and frequency-specific effects of transcranial alternating current stimulation are explained by network dynamics. J Neural Eng, 21(2), 026024. https://doi.org/10.1088/1741-2552/ad37d9
- [76] Markram H, Muller E, Ramaswamy S, Reimann MW, Abdellah M, Sanchez CA, et al. (2015). Reconstruction and simulation of neocortical microcircuitry. Cell, 163, 456-92. https://doi.org/10.1016/j.cell.2015.09.029
- [77] Huang X, Wei X, Wang J, Yi G. (2025). Multi-scale model of neural entrainment by transcranial alternating current stimulation in realistic cortical anatomy. J Comput Neurosci. https://doi.org/10.1007/s10827-025-00912-7
- [78] Aberra AS, Wang B, Grill WM, Peterchev AV. (2020). Simulation of transcranial magnetic stimulation in head model with morphologically-realistic cortical neurons. Brain Stimul, 13(1), 175-189. https://doi.org/10.1016/j.brs.2019.10.002
- [79] Dura-Bernal S, Griffith EY, Barczak A, O'Connell MN, Mc-Ginnis T, Moreira JVS, et al. (2023). Data-driven multiscale model of macaque auditory thalamocortical circuits reproduces in vivo dynamics. Cell Rep, 42(11), 113378. https://doi.org/10.1016/j.celrep.2023.113378
- [80] Yokota T, Maki T, Nagata T, Murakami T, Ugawa Y, Laakso I, et al. (2019). Real-time estimation of electric fields induced by transcranial magnetic stimulation with deep neural networks. Brain Stimul, 12(6), 1500-1507. https://doi.org/10.1016/j.brs.2019.06.015
- [81] Li H, Deng ZD, Oathes D, Fan Y. (2022). Computation of transcranial magnetic stimulation electric fields using self-supervised deep learning. Neuroimage, 264, 119705. https://doi.org/10.1016/j.neuroimage.2022.119705
- [82] Aberra AS, Lopez A, Grill WM, Peterchev AV. (2023). Rapid estimation of cortical neuron activation thresholds by transcranial magnetic stimulation using convolutional neural networks. Neuroimage, 275, 120184. https://doi.org/10.1016/j.neuroimage.2023.120184
- [83] Beniaguev D, Segev I, London M. (2021). Single cortical neurons as deep artificial neural networks. Neuron, 109(17), 2727-2739.e3. https://doi.org/10.1016/j.neuron.2021.07.002

[84] Yamins DL, DiCarlo JJ. (2016). Using goal-driven deep learning models to understand sensory cortex. Nat Neurosci, 19(3), 356-65. https://doi.org/10.1038/nn.4244